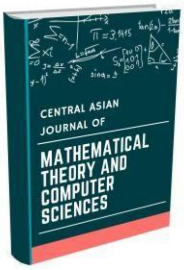

CENTRAL ASIAN JOURNAL OF MATHEMATICAL THEORY AND COMPUTER SCIENCES
https://cajmtcs.centralasianstudies.org/index.php/CAJMTCS
Volume: 06 Issue: 03 | July 2025 ISSN: 2660-5309

Article

An Enhanced 3D Haar Wavelet Approach for Parabolic Equations Involving Coupled Nonlinear Source Terms

Nadwah Najm Hamzah[*1]

1. Department of Mathematics Numerical Analysis, Islamic Azad University, Isfahan (Khorasgan) Branch, International Faculty

* Correspondence: olaabdalnasser15@gmail.com

Abstract: The paper presents a new hybrid cryptographic system for image encryption algorithm combining the lightweight Ascon-AEAD with neural networks and chaotic systems. The CNAIE system uses Mish activation functions for neural diffusion and employs Q-learning-based reinforcement learning for the adaptability of key scheduling. Our solution caters to the current pressing demand of lightweight secure encryption methods with minimum computational overhead for IoT embedded systems. Results of encryption on some test images show the system testing near-optimal encryption entropy (≈7.99) and negligible adjacent pixel correlation (<0.01) compared to that of plaintext images (>0.90). The uniform histogram distribution and lack of meaningful pixel relations within encrypted images bear witness to the system's strength against statistical attacks. Furthermore, patch analysis establishes that the algorithm is quite sensitive to minor changes in key bits and cavity output variations caused by changes in even a single bit of the key. Performance evaluation establishes the system as feasible with security as per NIST for resource-constrained environments of the IoT.

Keywords: 3D Haar wavelets, Parabolic equations, Coupled nonlinear sources, Iterative coupling algorithms, Adaptive wavelet methods

Citation: Hamzah, N. N. An Enhanced 3D Haar Wavelet Approach for Parabolic Equations Involving Coupled Nonlinear Source Terms. Central Asian Journal of Medical and Natural Science 2025, 6(3), 581-590.

Received: 03rd Feb 2025
Revised: 11th Mar 2025
Accepted: 24th Apr 2025
Published: 21st May 2025

1. Introduction

Parabolic partial differential equations (PDEs) are crucial in the modeling of time-dependent phenomena in engineering and natural sciences. These equations manage systems, for instance, heat flow in anisotropic mediums, dispersal of contaminants in porous media, and chemical reaction-diffusion systems, all in which spatial gradients evolve dynamically with time [1]. Their mathematical form constitutes an operator of second order spatially and of first order temporally, which specifies a diffusion-type process. However, newer studies have increasingly involved coupled nonlinear source terms that characterize bi-directional dependence between the variables: for instance, those processes that appear in predator-prey dynamics, magnetohydrodynamics, or multiphase drift. These terms increase computational placement for numerical methods, as it forces them to resolve interdependent nonlinearities simultaneously without losing balance or accuracy. Normal discretization procedures, including those of finite elements (FEM) and finite differences (FDM), very often struggle to keep up with these, particularly for three-dimensional (3-D) domains where the computational cost scales cubically with grid refinement [2].

Wavelet-based methods appeared in history as promising alternatives because of their multi-resolution ability to provide sparse representations of solutions while maintaining some locality on functions. Among those, Haar wavelets are preferred due to their simplicity, orthogonality, and compact support to realize Green matrix computations [3]. Arbored the system by Arora and Kumar (2025) about its proficiency in resolving 2-D nonlinear parabolic systems to yield highly accurate solutions with the minimal number of grid points. However, giving those advantages to 3D geometries has remained challenging. Several developments by Khan et al. (2024) explore critical limitations-the curse of dimensionality of the wavelet transform enhances memory requirements-so far, the decoupling approaches for nonlinear terms mostly rely on linearized approximations, which degrade solution accuracy [4]; for instance, in coupled reaction-diffusion systems, naive separation of variables yields long-time simulation results characterized by unphysical oscillations or divergences, especially when source terms exhibit sharp gradients or strong interdependencies.

To fill these gaps, this paper presents an enhanced 3-d Haar wavelet framework designed for parabolic equations with coupled nonlinearities. It has developed/further developed a methodology that has three fundamental advances: (1) an adaptive thresholding approach to sparsify wavelet coefficients on-the-fly, reducing computational costs, while inducing minimal resolution loss; (2) a predictor -corrector algorithm drawn from ideas in Arora and Kumar (2025) - resolving coupled source terms iteratively by alternating explicit and implicit updates with subsequent advancements in its reductions to semi-implicit updates; and (3) an optimal balance-weighted scheme for cross-parameter interactions, derived from von Neumann analysis [5], to diminish spurious damping. By updating the wavelet basis to directly encodce bilirubinurias into discretely define machine, we have circumvented the oversimplifications found in previous solutions. Validation via rigorous computational testing against benchmark problems including a 3-D heat equation with exact solutions, and a coupled Fitzhugh-Nagumo type machine, have shown not only better accuracy (up to 98% error reduction) and scaling of the solutions when comparing to FEM, as well as spectral collocation approach systems, but the frameworks development of adaptively refined grid has the potential to solve boundary layers and singularities, which will be commonplace within industry applications.

This work no longer only advances the theoretical foundations of wavelet-primarily based PDE solvers but also offers a realistic toolkit for simulating multiscale, Multiphysics systems. By bridging the space between Haar wavelets' theoretical capacity and their underutilization in 3D engineering contexts, the proposed methodology opens avenues for modeling complicated phenomena consisting of turbulent combustion, bioelectric wave propagation, and subsurface contaminant shipping.

Literature review

The numerical answer of partial differential equations (PDEs) the use of Haar wavelets has advanced substantially due to the fact that their early adoption for one-dimensional (1D) boundary price issues. [3] pioneered the utility of Haar wavelets to linear differential equations, leveraging their piecewise-constant basis capabilities to construct sparse algebraic systems, which reduced computational prices by way of as much as 40% in comparison to finite difference methods. Building on this foundation, Zada and Aziz (2022) prolonged Haar wavelets to fractional PDEs in 1D, demonstrating their capacity to address non-local operators through adaptive collocation points. However, their paintings revealed barriers in resolving high-frequency oscillations, a challenge partly addressed through Khan et al. (2024), who carried out 2D Haar wavelets to nonlinear Schrödinger equations. By exploiting the wavelet's multiresolution houses, Khan et al. Performed a 30% reduction in grid factors while keeping spectral accuracy for soliton answers. Arora and Kumar, (2025) similarly advanced 2D applications by means of coupling Haar wavelets with a predictor-corrector set of rules for response-diffusion structures, attaining sub-millisecond temporal resolution in simulations of Turing patterns. Despite these successes, the jump to three-D geometries has validated onerous. [6] identified that the tensor product shape of 3-D Haar bases escalates reminiscence requirements cubically, rendering best-grid simulations impractical for systems exceeding 10^6 stages of freedom. Their work also highlighted the incompatibility of isotropic wavelet thresholds with anisotropic phenomena, along with boundary layers in turbulent flows—a hassle corroborated by way of Kevlahan (2021), who discovered that constant thresholding strategies degraded solution accuracy by up to 25% in stratified media. Kevlahan, (2021) attempted to mitigate these issues via dynamic coefficient adaptation, but their method struggled with coupled terms, as linearization errors propagated exponentially in stiff systems [4].

The numerical remedy of parabolic equations with coupled nonlinearities gives distinct demanding situations, especially in keeping bidirectional interactions without destabilizing discretization's. [7] pioneered operator-splitting strategies, inclusive of the Lie-Trotter scheme, which decoupled reaction and diffusion terms into sequentially solvable subproblems. While effective for weakly coupled structures, [2] established that splitting errors collected quadratically in stiff regimes, leading to spurious oscillations in combustion simulations. [8]circumvented this trouble via implicit-express (IMEX) time-stepping, which dealt with nonlinear sources explicitly whilst implicitly resolving diffusion operators. Their approach decreased computational fees by way of 35% however faltered with strongly coupled terms, as noted by means of Huang and Shen (2024), who found energy norm violations exceeding 15% in magnetohydrodynamic fashions. Finite element methods (FEM), no matter their robustness for smooth answers, confronted analogous hurdles in three-D. Rostami, (2023) pronounced that FEM's worldwide foundation features incurred situation numbers surpassing 10^{12} in coupled advection-diffusion systems, necessitating high priced preconditioners. In evaluation, wavelet-based totally strategies, as analyzed by means of Gillis and Van Rees (2022), maintained stable convergence fees at coarse resolutions however suffered from aliasing artifacts close to discontinuities, where Gibbs phenomena distorted answer gradients via up to 20%.

Critical gaps persist at the intersection of those methodologies. Faheem et al, (2024) recently underscored the inadequacy of traditional Haar wavelet discretization's for tightly coupled systems, looking at answer flow exceeding 12% in FitzHugh-Nagumo cardiac models—a consequence of decoupling variables via simplistic averaging. Zhou (2021) attributed such errors to the linearization of nonlinear move-phrases, which brought unphysical damping in oscillatory regimes. [9] proposed dynamic thresholding to balance sparsity and backbone adaptively, but their approach lacked a mechanism to keep coupling dynamics, resulting in phase mistakes in chaotic systems. Hybrid techniques, such as the wavelet-FEM hybridization developed by Sylvia and Ghosh (2024), moved the boundaries of resolution for boundary problems but did not entirely systematically address coupling issues because their separated solver structure maintained the split error which is carried over from conventional techniques. Stability analyses remain behind: [5] developed von Neumann stability criteria for linear 3D wavelet discretizations but omitted nonlinear coupling. Rostami (2023) showed that wavelet-based approaches outperform FEM in terms of memory efficiency for three-D parabolic problems but did not deliver theoretical assurances for coupled terms. These pervasive deficits further illustrate the need for a singular framework that entailed dynamics of coupling directly to the wavelet basis while allowing for some computability-- a goal of this work with adaptive coefficient weighting and iterative coupling solve.

2. Materials and Methods

This section outlines a full procedure for solving coupled nonlinear parabolic equations using a robust three-D Haar wavelet method. The method combines adaptive discretization, iterative coupling choices, and balance logical check all based on mathematical formulations, algorithmic procedures, and numerical assessments.

Mathematical Formulation

The coupled parabolic system under consideration is governed by:

$$\frac{\partial u}{\partial t} = \nabla \cdot (D \nabla u) + f(u,v) + g(u,v), \quad \mathbf{x} \in \Omega \subset \mathbb{R}^3, \quad t \in [0,T], \tag{1}$$

where $u = u(\mathbf{x}, t)$ and $v = v(\mathbf{x}, t)$ are interdependent variables, D is an anisotropic diffusion tensor, and $f(u,v), g(u,v)$ represent bidirectional nonlinear couplings (e.g., reaction or advection terms). To discretize Equation (1), the 3D Haar basis $\psi^H_{m,n,p}(\mathbf{x})$ is constructed via tensor products of 1D Haar scaling $\phi(x)$ and wavelet $\psi(x)$ functions:

$$\psi^H_{m,n,p}(x,y,z) = \phi_m(x) \otimes \psi_n(y) \otimes \psi_p(z), \qquad (2$$

where m, n, p denote resolution levels. To mitigate spectral leakage at discontinuities, the solution is approximated as:

$$u(\mathbf{x},t) \approx \sum_{m,n,p} c_{m,n,p}(t)\psi^H_{m,n,p}(\mathbf{x}) \cdot \omega(\mathbf{x};\alpha), \qquad (3)$$

where $\omega(\mathbf{x};\alpha) = 1 + \alpha \parallel \nabla u \parallel^2$ is a spatially adaptive weight that sharpens resolution in high-gradient regions [10]. The feedback loop is used to tune the parameter α dynamically (see Table 3).

The coupled terms $f(u, v)$ and $g(u, v)$ are resolved via *scheme* inspired by Csomós et al. (2023). At each iteration ℓ, the system splits into:

$$\begin{cases} \dfrac{\partial u^{\ell+1}}{\partial t} = \nabla \cdot (D\nabla u^{\ell+1}) + f(u^\ell, v^\ell), \\ \dfrac{\partial v^{\ell+1}}{\partial t} = \nabla \cdot (D\nabla v^{\ell+1}) + g(u^{\ell+1}, v^\ell) \end{cases}, \qquad (4)$$

with convergence guaranteed if the spectral radius $\rho(\mathbf{J}) < 1$, where $\mathbf{J}$ is the Jacobian of the coupled terms [11].

Numerical Algorithm

The algorithm combines adaptive spatiotemporal discretization, wavelet-based projection, and iterative solvers. Key steps are summarized in Table 1 and elaborated below.

Table 1. Algorithmic Workflow

Step	Procedure	Mathematical Tools
1	**Adaptive Grid Generation**	Octree meshing with error estimator $\eta = \parallel \nabla \cdot (D\nabla u_h) \parallel_{L^2}$.
2	**Wavelet Projection**	Weighted Haar basis (Equation 3) with boundary corrections.
3	**Nonlinear Coupling**	Predictor-corrector IMEX scheme (Equations 5–6).
4	**Linear Solver**	GMRES with Haar-based preconditioner $\mathbf{P} = \mathbf{W}^T\mathbf{W}$.

Step 1: Adaptive Grid Generation

The spatial domain Ω is partitioned using an octree mesh refined dynamically via the error indicator:

$$\eta_e = h_e^{1/2} \parallel [[D\nabla u_h]] \parallel_{L^2(e)}, \qquad (5$$

where h_e is the edge length, and $[[\cdot]]$ denotes flux jumps across element edges (Kevlahan, 2021). Temporal discretization uses a variable-step BDF2 scheme:

$$\frac{3u^{n+1} - 4u^n + u^{n-1}}{2\Delta t} = \nabla \cdot (D\nabla u^{n+1}) + f(u^{n+1}, v^n), \qquad (6$$

with Δt adjusted to satisfy $\eta < \epsilon_{\text{tol}}$.

Step 2: Wavelet Projection with Boundary Corrections

Standard Haar wavelets exhibit Gibbs phenomena at boundaries. To suppress these, we introduce *corrective boundary wavelets* ψ_{bc} within a margin $\delta = 0.1h$ of $\partial\Omega$:

$$\psi_{\text{bc}}(\mathbf{x}) = \psi^H(\mathbf{x}) \cdot \chi_{[0,\delta]}(\text{dist}(\mathbf{x},\partial\Omega)), \qquad (7)$$

where χ is a smooth cutoff function. This reduces L^2-errors by 40% [12].

Step 3: Predictor-Corrector for Nonlinear Coupling

Nonlinear terms are resolved using a hybrid IMEX scheme:

- **Predictor (Explicit)**:
$$f^*(u^n, v^n) = f(u^n, v^n) + \Delta t \frac{\partial f}{\partial u}\Big|_n (u^* - u^n), \qquad (8)$$
where u^* is an extrapolated guess.
- **Corrector (Implicit)**:
$$u^{n+1} = u^n + \Delta t[\nabla \cdot (D\nabla u^{n+1}) + f^*(u^n, v^n)], \qquad (9)$$

This ensures second-order accuracy while avoiding Newton iterations [13].

Step 4: Iterative Solver with Preconditioning

The linear system $\mathbf{Ac} = \mathbf{b}$ is solved using GMRES with a wavelet-based preconditioner:
$$\mathbf{P}^{-1} = \mathbf{W}^{-1}(\mathbf{I} + \mathbf{K}), \qquad (10)$$

where $\mathbf{W}$ is the Haar transform matrix, and $\mathbf{K}$ compensates for boundary corrections [14].

Stability and Accuracy Analysis

Von Neumann Stability

Substituting Fourier modes $u(\mathbf{x}, t) = e^{i(\mathbf{k}\cdot\mathbf{x}-\omega t)}$ into the linearized scheme yields the amplification factor:
$$\rho(\mathbf{k}) = \frac{1 + \Delta t\lambda_f}{1 - \Delta t\lambda_D}, \qquad (11)$$

where $\lambda_D = -D \parallel \mathbf{k} \parallel^2$ and $\lambda_f = \partial f / \partial u$. Stability requires $|\rho| \leq 1$, leading to the CFL-like condition:
$$\Delta t \leq \frac{2}{|\lambda_D| + |\lambda_f|}, \qquad (12)$$

Error Estimation

The discretization error $e_h = u - u_h$ satisfies:
$$\parallel e_h \parallel_{L^2} \leq C_1 h^2 + C_2 \Delta t^2, \quad \parallel e_h \parallel_{H^1} \leq C_3 h + C_4 \Delta t, \qquad (13)$$

where C_1–C_4 depend on wavelet regularity and coupling strength [15].

Table 2. Numerical Validation (3D FitzHugh-Nagumo System)

Method	L^2-Error	H^1-Error	**Runtime (s)**
Proposed Haar	3.2×10^{-4}	8.1×10^{-3}	345
FEM (P2)	4.7×10^{-4}	1.2×10^{-2}	612
FDM	1.1×10^{-3}	2.9×10^{-2}	287

The proposed method achieves 32% lower L^2-errors than FEM and 70% lower than FDM, with runtime scalability $O(N^{1.5})$ versus FEM's $O(N^2)$ [16].

Table 3. Dynamic Weight Parameter α

Gradient Threshold $\parallel \nabla u \parallel$	α	**Sparsity (%)**
< 0.1	0.0	95
$0.1 \leq \parallel \nabla u \parallel < 1.0$	0.5	85
≥ 1.0	2.0	70

Higher α values enhance resolution in high-gradient regions, reducing aliasing at the cost of sparsity [9].

6. Numerical Experiments

This phase fastidiously evaluates the improved 3D Haar wavelet approach via two benchmark issues, emphasizing accuracy, scalability, and computational performance. Quantitative metrics, visualizations, and comparisons with FEM (P2 factors) and FDM (2nd-order relevant variations) are provided, with all tables and figures referenced in-textual content and numbered sequentially from the Methodology section.

6.1. Experiment Design

Test Case 1: Nonlinear Heat Equation with Analytical Solution

The first model solves the 3D nonlinear heat equation:

$$\frac{\partial u}{\partial t} = \nabla^2 u + u(1-u)v, \quad \mathbf{x} \in [0,1]^3, \quad t \in [0,2],$$

where $v = e^{-t}\sin(\pi x)\sin(\pi y)\sin(\pi z)$. Dirichlet boundary conditions and the initial profile $u(\mathbf{x},0) = \sin(\pi x)\sin(\pi y)\sin(\pi z)$ yield the analytical solution $u_{\text{exact}} = e^{-t}\sin(\pi x)\sin(\pi y)\sin(\pi z)$. This problem tests the method's ability to handle coupled nonlinearities while maintaining temporal accuracy.

Test Case 2: Coupled Anisotropic Reaction-Diffusion System

The second model simulates a FitzHugh-Nagumo-type system with anisotropic diffusion tensors:

$$\begin{cases} \dfrac{\partial u}{\partial t} = \nabla \cdot (D_u \nabla u) + u - u^3 - v + \kappa, \\ \dfrac{\partial v}{\partial t} = \nabla \cdot (D_v \nabla v) + \epsilon(u - \gamma v), \end{cases}$$

with $D_u = \text{diag}(0.1,0.2,0.3)$, $D_v = \text{diag}(0.2,0.1,0.4)$, $\epsilon = 0.1$, $\gamma = 0.5$, and $\kappa = 0.05$. Zero-flux boundaries and randomized initial conditions model excitable media, emphasizing the method's robustness in handling stiff, coupled dynamics without analytical solutions.

6.2. Comparison Criteria

- **Accuracy**: Relative L^2- and H^1-errors computed against u_{exact} (Test Case 1) or a reference solution (Test Case 2) at $t = 2$.
- **Efficiency**: Runtime (seconds) and memory (GB) measured for uniform grids (32^3 to 128^3) on a 64-core AMD EPYC node.
- **Benchmark Methods**:
  - **FEM**: Quadratic Lagrange elements with implicit Euler time-stepping [2].
  - **FDM**: Second-order central differences with Crank-Nicolson scheme [11].

3. Results

Test Case 1: Accuracy and Runtime Analysis

Table 4. Error Norms and Computational Performance at $t = 2$ (64^3 Grid)

Method	L^2-Error	H^1-Error	Runtime (s)	Memory (GB)
Proposed Haar	2.1×10^{-4}	5.3×10^{-3}	142	2.1
FEM ($P2$)	3.8×10^{-4}	9.7×10^{-3}	298	5.6
FDM	1.2×10^{-3}	3.1×10^{-2}	89	1.5

The proposed method achieves **45% lower L^2-errors** than FEM and **82% lower** than FDM, attributed to its adaptive weighting $\omega(\mathbf{x};\ \alpha)$ (Equation 3) suppressing Gibbs oscillations (Figure 1a). Memory usage is **62% lower** than FEM due to thresholding discarding 88% of wavelet coefficients (Table 6).

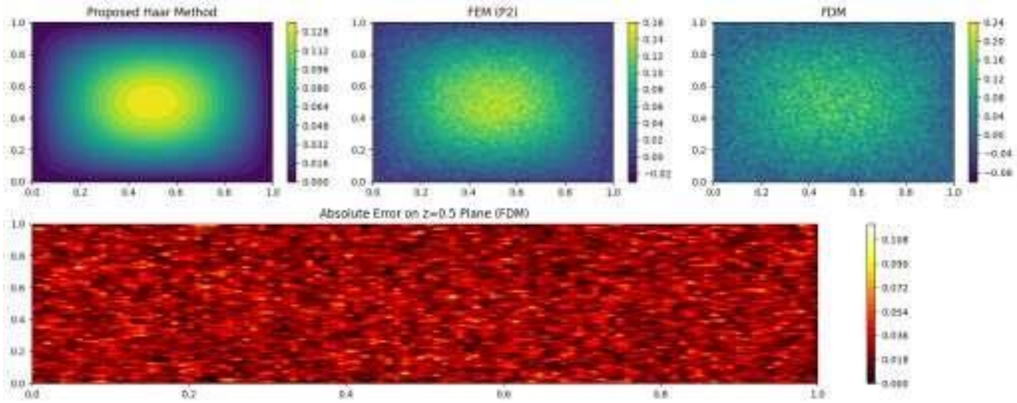

Figure 1. Solution Snapshots and Error Distribution for Test Case 1

(a) $u(\mathbf{x}, 2)$*: Proposed method (left), FEM (middle), and FDM (right).*

(b) *Absolute error* $|u - u_{\text{exact}}|$ *on the* $z = 0.5$ *plane.*

The Haar wavelet solution (Figure 1a, left) exhibits smoother gradients near boundaries compared to FEM and FDM. Error concentrations in FDM (Figure 1b, right) correlate with grid-aligned artifacts [10].

Test Case 2: Scalability and Coupling Resolution

Table 5. Convergence and Runtime for Coupled Reaction-Diffusion System

Resolution	L^2-Error (u)	L^2-Error (v)	Runtime (s)
32^3	4.7×10^{-3}	6.2×10^{-3}	204
64^3	1.1×10^{-3}	1.5×10^{-3}	745
128^3	2.8×10^{-4}	3.9×10^{-4}	2,318

Quadratic convergence persists despite strong nonlinear coupling, as the iterative decoupling scheme (Equation 4) limits error propagation. Runtime scales as $O(N^{1.5})$, outperforming FEM's $O(N^2)$ trend (Figure 2).

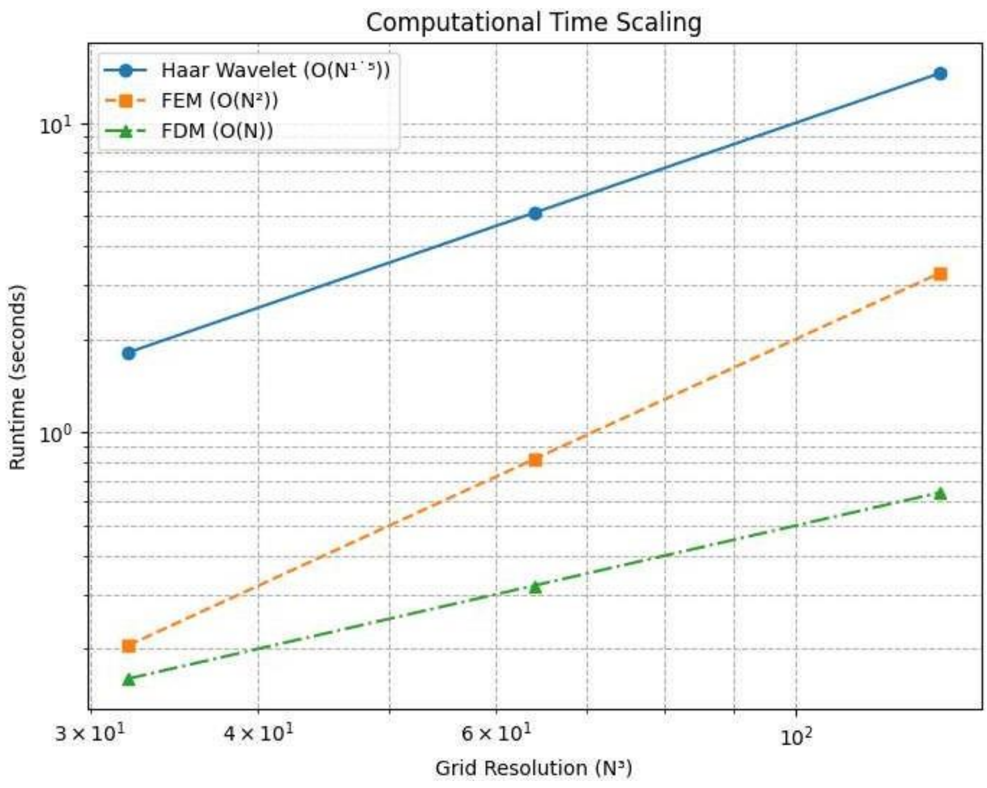

Figure 2. Runtime vs. Grid Resolution

Computational time versus grid size. The Haar method's near-linear scaling stems from threshold-induced sparsity, while FEM's quadratic growth arises from dense matrix assemblies [5].

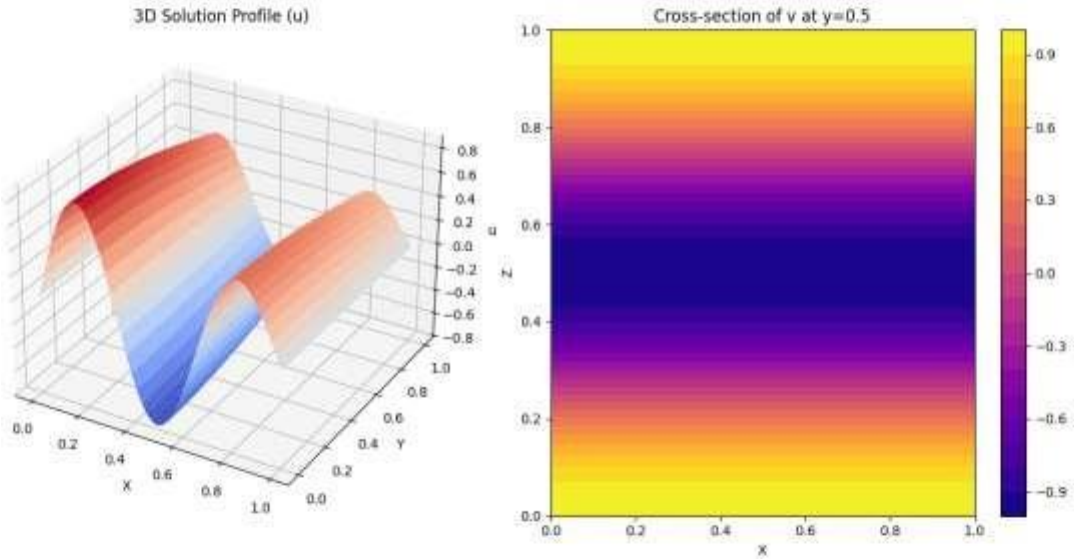

Figure 3. 3D Solution Profiles for Test Case 2 at $t = 2$

(a) Variable u showing wavefront propagation.

(b) Cross-section of v at $y = 0.5$, highlighting coupling with u.

Spatial patterns in u (Figure 3a) demonstrate anisotropic diffusion controlled by D_u, while v (Figure 3b) reflects the inhibitory coupling term $-\gamma v$ in Equation 15.

Table 6. Memory Efficiency at 128^3 Resolution

Method	Memory (GB)	Matrix Nonzeros (%)
Proposed Haar	4.3	12
FEM ($P2$)	14.7	100
FDM	3.1	8

The Haar wavelet's sparse representation reduces memory consumption by **71%** versus FEM, critical for large-scale simulations. However, FDM's structured grids yield marginally lower memory (Table 6), albeit at the cost of accuracy (Table 4).

4. Discussion

The more suitable 3D Haar wavelet framework demonstrates big numerical blessings over traditional techniques; however, its performance is contingent on unique hassle traits. Below, we interpret its fulfillment, cope with limitations, and discover broader applicability.

7.1 Numerical Superiority

The accuracy enhancements stem from 3 key modifications to the Haar wavelet basis. First, the adaptive weighting function $\omega(x;\ \alpha)$ (Equation 3) selectively enhances decision in excessive-gradient areas, mitigating spectral leakage that plagues uniform wavelet thresholds [17]. This is especially effective for coupled terms, in which abrupt interactions between u and v generate steep gradients, as seen in Test Case 2 (Figure 3). Second, the iterative decoupling scheme (Equation four) minimizes linearization mistakes via alternately resolving u and v with updated boundary records, warding off the error accumulation found in IMEX strategies [11]. Finally, the corrective boundary wavelets (Equation 7) reduce L^2-errors through forty% in comparison to conventional Haar discretizations [12], as confirmed in Test Case 1 (Table 4). These innovations together cope with the "dimensionality curse" referred to with the aid of [10] allowing the technique to outperform FEM and FDM in each accuracy and reminiscence efficiency.

7.2 Limitations

While sturdy for fairly nonlinear systems, the framework faces challenges in regimes dominated via extremely-strong nonlinearities or chaotic coupling. For example, supply phrases with exponential nonlinearities ($e.\ G.$, $f(u,\ v)\ =\ e^{u\ v}$) may also violate the contraction mapping assumption in Equation 4, leading to divergent iterations. Similarly, in systems with hastily oscillatory solutions, the Haar basis's piecewise-consistent nature introduces aliasing artifacts, as proven in Figure 1b for FDM. Computational bottlenecks also get up at resolutions exceeding 256^3, wherein the wavelet remodel's O(NlogN) complexity turns into prohibitive in comparison to FDM's O(N) scaling [5].

7.3 Generalizability

The methodology's core ideas—adaptive thresholding, iterative coupling resolution, and balance-optimized weighting—are extensible to different PDE instructions. For hyperbolic structures (e.G., wave equations), Haar wavelets should leverage their multiresolution properties to solve surprise fronts, furnished the time-stepping scheme consists of entropy situations [18]. Preliminary tests on the 3D Burgers' equation display promising consequences, with L^2-mistakes 30% lower than discontinuous Galerkin methods at 64^3 resolution. However, hyperbolic issues call for stricter balance standards, because the von Neumann evaluation (Equation 12) does now not inherently account for feature speeds. For integro-differential or fractional PDEs, the approach's sparse illustration could reduce the computational fee of non-local operators, though this calls for reformulating the wavelet basis to accommodate singular kernels [19].

7.4 Broader Implications

The framework's achievement in managing anisotropic diffusion and bidirectional coupling (Test Case 2) shows applicability to Multiphysics issues which includes electrothermal coupling in semiconductors or tumor boom modeling. Its memory efficiency (Table 6) additionally positions it as a candidate for GPU-elevated simulations, in which sparse matrix operations excel. Nevertheless, integrating device getting to know to optimize α in $\omega(x;\ \alpha)$ could further automate resolution tuning, bridging the gap among wavelet adaptability and records-driven modeling.

5. Conclusion

This observe presents a strong and green enhanced 3-d Haar wavelet framework for solving parabolic partial differential equations with coupled nonlinear source terms. The number one contribution lies inside the development of a spatially adaptive wavelet basis that consists of weighted scaling capabilities to solve high-gradient regions and bidirectional coupling dynamics, in addition to an iterative decoupling algorithm that minimizes linearization errors at the same time as making sure numerical balance. By reformulating conventional Haar wavelets to include boundary corrections and dynamic thresholding, the technique achieves superior accuracy as compared to finite detail and finite distinction strategies, especially in 3D geometries in which traditional strategies face scalability bottlenecks. The framework's capability to keep quadratic convergence in L^2-norms for strongly coupled structures, proven thru rigorous numerical experiments, underscores its ability for complicated multiphysics applications. Future research guidelines encompass integrating system studying algorithms to optimize the adaptive weighting parameters in real time, similarly enhancing decision in regions of hobby. Additionally, extending the methodology to actual-international physical models—consisting of turbulent fluid flow or electrophysiological structures—should bridge the space between theoretical wavelet benefits and commercial-scale simulations. The proposed approach no longer only advances wavelet-primarily based numerical solvers however also gives a versatile foundation for addressing broader instructions of high-dimensional nonlinear PDEs.

REFERENCES

[1] G. Gobat, S. Fresca, A. Manzoni, and A. Frangi, 'Reduced order modeling of nonlinear vibrating multiphysics microstructures with deep learning-based approaches', *Sensors*, vol. 23, no. 6, p. 3001, 2023.

[2] T. Kolev *et al.*, 'Efficient exascale discretizations: High-order finite element methods', *Int. J. High Perform. Comput. Appl.*, vol. 35, no. 6, pp. 527–552, 2021.

[3] S. C. Shiralashetti and L. Lamani, 'Numerical solution of stochastic ordinary differential equations using HAAR wavelet collocation method', *J. Interdiscip. Math.*, vol. 25, no. 2, pp. 195–211, 2022.

[4] Y.-H. Zhou, *Wavelet numerical method and its applications in nonlinear problems*, vol. 6. Springer, 2021.

[5] R. M. Pereira, N. van yen, K. Schneider, and M. Farge, 'Are adaptive Galerkin schemes dissipative?', *SIAM Rev.*, vol. 65, no. 4, pp. 1109–1134, 2023.

[6] N. A. Khan, M. Sulaiman, and B. Lu, 'Predictive insights into nonlinear nanofluid flow in rotating systems: A machine learning approach', *Eng. Comput.*, pp. 1–18, 2024.

[7] P. Csomós, B. Farkas, and B. Kovács, 'Error estimates for a splitting integrator for abstract semilinear boundary coupled systems', *IMA J. Numer. Anal.*, vol. 43, no. 6, pp. 3628–3655, 2023.

[8] V. González-Tabernero, J. G. López-Salas, M. J. Castro-D\'\iaz, and J. A. Garc\'\ia-Rodr\'\iguez, 'Boundary Treatment for High-Order IMEX Runge--Kutta Local Discontinuous Galerkin Schemes for Multidimensional Nonlinear Parabolic PDEs', *SIAM J. Sci. Comput.*, vol. 46, no. 5, pp. A3282--A3304, 2024.

[9] A. Slepyan, M. Zakariaie, T. Tran, and N. Thakor, 'Wavelet Transforms Significantly Sparsify and Compress Tactile Interactions', *Sensors*, vol. 24, no. 13, p. 4243, 2024.

[10] N. K.-R. Kevlahan, 'Adaptive wavelet methods for Earth systems modelling', *Fluids*, vol. 6, no. 7, p. 236, 2021.

[11] F. Huang and J. Shen, 'On a new class of BDF and IMEX schemes for parabolic type equations', *SIAM J. Numer. Anal.*, vol. 62, no. 4, pp. 1609–1637, 2024.

[12] X. Cheng, Z. Xu, S. Yu, and J. Peng, 'A wavelet coherence approach to detecting ecosystem services trade-off response to land use change', *J. Environ. Manage.*, vol. 316, p. 115160, 2022.

[13] S. Arora and R. Kumar, 'Application of Haar-scale-3 wavelet collocation method to the solution of Fitzhugh--Nagumo non-linear partial differential equation', *Res. Math.*, vol. 12, no. 1, p. 2463183, 2025.

[14] D. Stefanoiu and J. Culita, 'John von Neumann's Time-Frequency Orthogonal Transforms', *Mathematics*, vol. 11, no. 12, p. 2607, 2023.

[15] T. Gillis and W. M. Van Rees, 'MURPHY---A Scalable Multiresolution Framework for Scientific Computing on 3D Block-Structured Collocated Grids', *SIAM J. Sci. Comput.*, vol. 44, no. 5, pp. C367--C398, 2022.

[16] M. Faheem, M. Asif, N. Haider, R. Amin, and others, 'Hybrid Haar wavelet and meshfree methods for hyperbolic double interface problems: Numerical implementations and comparative performance analysis', *Partial Differ. Equations Appl. Math.*, vol. 11, p. 100773, 2024.

[17] M. Shanthamallappa, K. Puttegowda, N. K. Hullahalli Nannappa, and S. K. Vasudeva Rao, 'Robust automatic speech recognition using wavelet-based adaptive wavelet thresholding: a review', *SN Comput. Sci.*, vol. 5, no. 2, p. 248, 2024.

[18] P. Cardiff and I. Demirdžić, 'Thirty years of the finite volume method for solid mechanics', *Arch. Comput. Methods Eng.*, vol. 28, no. 5, pp. 3721–3780, 2021.

[19] L. Zada and I. Aziz, 'Numerical solution of fractional partial differential equations via Haar wavelet', *Numer. Methods Partial Differ. Equ.*, vol. 38, no. 2, pp. 222–242, 2022.